Enhanced nonlinear optical response of InP(100) membranes

M. Reid, I. Cravetchi, and R. Fedosejevs*

Department of Electrical and Computer Engineering, University of Alberta, Edmonton T6G 2V4, Canada

I. M. Tiginyanu and L. Sirbu

Laboratory of Low Dimensional Semiconductor Structures, Institute of Applied Physics,
Academy of Sciences and Technical University of Moldova, 2004 Chisianau, Moldova

Robert W. Boyd

Institute of Optics, University of Rochester, Rochester, New York 14627, USA

The nonlinear optical response of porous InP(100) membranes was examined and compared to that of bulk crystalline (100)-oriented InP. Measurements of optical rectification and optical second-harmonic generation have been carried out in reflection under excitation by 120 fs, 800 nm Ti:Sapphire laser beam pulses. A significant enhancement in both the radiated terahertz field and second-harmonic radiation from the porous InP(100) surface, relative to the bulk InP(100) surface, was observed. Terahertz field polarization measurements indicate that the enhancement is primarily on the component of the radiated field related to optical rectification as opposed to photocarrier-related effects. It is suggested that the enhanced nonlinear optical response is related to strong enhancements of the local field within the porous network.

PACS number(s): 42.65.Ky, 42.70.Mp

Porous III-V semiconductors offer a potentially attractive alternative to bulk semiconductors as a nonlinear medium exhibiting a strongly enhanced nonlinear optical response.[1–3] It was demonstrated experimentally that a 100-fold increase of the second-harmonic (SH) power could be achieved in porous, relative to bulk III-V semiconductors.[1,2] The observed enhancement factor is currently the subject of investigation, and has been attributed to such processes as local field enhancement within the porous network,[1] and an increased interaction of the radiation within the porous network due to scattering.[2,3]

In order to explore the effect of local field enhancement, we carried out investigations of the second-harmonic generation (SHG) from bulk and porous InP(100) in a reflection geometry, using pump radiation with photon energies greater than the band gap. The escape depth of the SH radiation limits the probed volume to a small depth, thus keeping scattering contributions to the enhancement to a minimum.

It is expected that the enhancement would also exist for the related phenomenon of optical rectification (OR), which would, in turn, lead to enhanced emission of pulsed terahertz (THz) radiation from InP surfaces. The THz emission is examined in the same reflection geometry, where a similar enhancement factor is observed for the THz radiation in comparison to SHG. The long wavelengths present in the THz radiation compared to the porous network skeleton feature size would minimize scattering contributions to the enhancement factor.

However, the comparison of SHG and OR has to be done carefully, as there are multiple mechanisms leading to the emission of THz radiation, the relative magnitudes of which are strongly dependent upon pump fluence.[4] To address this point, high-excitation fluences are used (1 mJ/cm²), where optical rectification is expected to dominate the THz emission. This is confirmed by measuring the polarization char-

acteristics of the THz radiation. The observation of increased THz emission from porous samples is also of importance to the THz community as application areas for pulsed THz radiation grow. In particular, emitters with improved efficiency are needed for THz imaging.[5,6]

Crystalline (100)-oriented substrates of n-InP with a 500-μm thickness and a free electron concentration of 1.3×10^{18} cm^{-3} were used. The electrochemical etching was carried out in 5% HCl aqueous solution in a potentiostatic regime to form the porous structure as described elsewhere.[7] A TESCAN scanning electron microscope (SEM) equipped with an energy dispersive x-ray (Oxford Instruments INCA EDX) system was used to analyze the morphology and chemical composition of the porous samples. Figure 1 shows a SEM image taken from a porous InP membrane. Note that
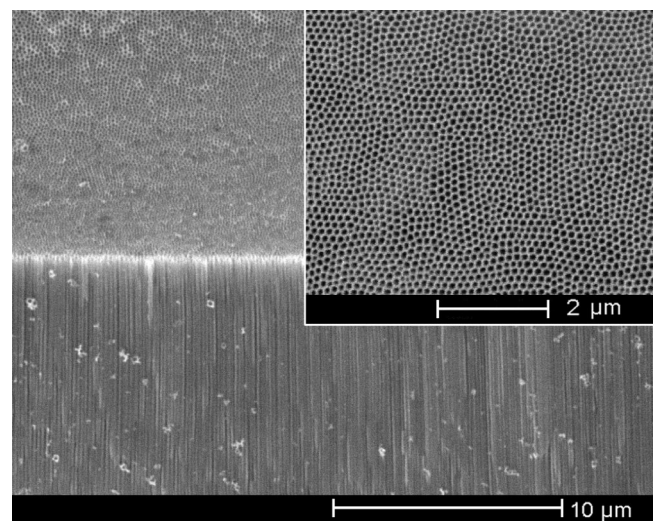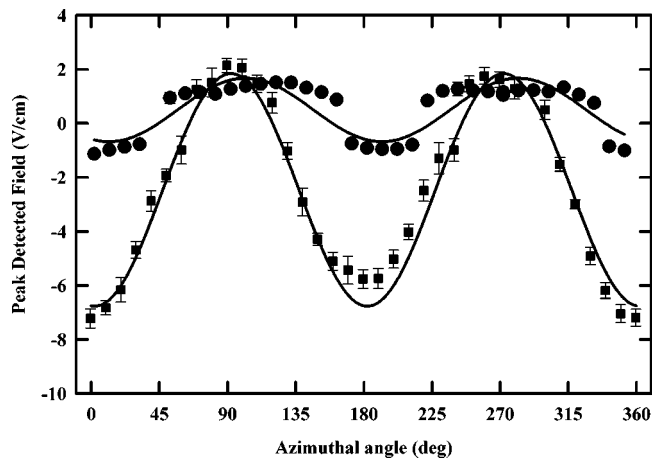

FIG. 1. SEM image of porous InP(100) membrane.

FIG. 2. Azimuthal dependence of the *p*-polarized THz field amplitude in reflection from the porous (squares) and bulk (circles) InP(100) samples under *p*-polarized excitation. Solid lines are qualitative fits to the data reflecting azimuthal dependence.
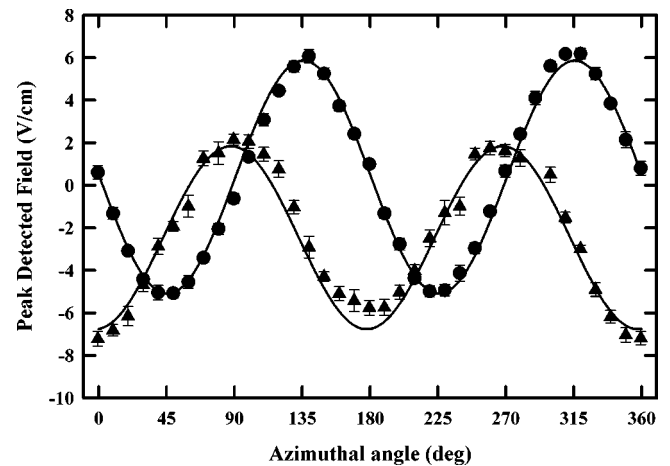

FIG. 3. Azimuthal dependence of the *p*-polarized (triangles) and *s*-polarized (circles) THz field amplitude in reflection from the porous InP(100) sample under *p*-polarized excitation. Solid lines are qualitative fits to the data reflecting azimuthal dependence.

pores with an average diameter of about 100 nm stretch perpendicular to the initial surface ($\pm 5°$ tolerance), leaving InP walls with an average thickness of about 50 nm, and extend up to 100 μm into the sample, which is deeper than the optical penetration depth of the pump beam used in the experiments (300 nm for InP at $\lambda = 800$ nm). The energy dispersive x-ray (EDX) microanalysis confirmed the stoichiometric composition of the InP skeleton.

The experimental setup for investigating the THz emission from bulk and porous InP is similar to that reported previously.[8] A regeneratively amplified Ti:Sapphire laser system (Spectra Physics Hurricane) is used as a pump source, operating at a center wavelength of 800 nm, at a 1-kHz repetition rate, with a maximum pulse energy of 750 μJ and a pulse width of 120 fs (Gaussian full width at half maximum). The beam is split into pump (92%) and probe (4%) beams using a wedged window. The probe pulse is delayed with respect to the pump using a scanning optical delay line. A variable attenuator ($\lambda/2$ plate and polarizer) is used in the pump beam to vary the fluence. The THz radiation from the surface of the sample oriented at a 45° angle of incidence is collected in the specular direction and imaged onto the ZnTe detector using four F/2 parabolic mirrors. A 1-mm-thick ZnTe (110) electrooptic crystal is used as detector/analyzer, oriented for sensitivity to *p*-polarized THz emission,[9] and can be reoriented to attain sensitivity to the *s*-polarized THz emission. A value of 3.9 pm/V is used for the linear electro-optic coefficient, to calculate the THz electric fields.[9]

The InP(100) samples were rotated about the surface normal, and the detected THz fields were measured as a function of the azimuthal angle ϕ, defined as the angle that the linearly *p*-polarized pump beam makes with the $[01\bar{1}]$ crystal axis in the (100) crystal plane. The samples were irradiated with an incident flux of approximately 1 mJ/cm^2 in a *p*-pol in-*p*-pol out polarization geometry (which we will refer to as a *p-p* geometry). The azimuthal dependencies of the THz field are shown in Fig. 2. Qualitative fits to the data of the form, $E_{THz} = a\cos(2\phi) + b$, are plotted together with the measured electric field. A change in polarity in the emitted electric field is observed from both samples as a function of the azimuthal angle. The observed angularly independent contribution to the radiated THz field may result from photocarrier effects,[10,11] however, it is inconsistent with bulk OR.[12] This issue will be discussed below. What is most apparent in Fig. 2 is that the peak-detected field from the bulk sample is approximately 1.6 ± 0.25 V/cm, while the peak-detected field from the porous InP(100) membrane is in excess of 7.0 ± 0.25 V/cm. Taking into account that the total emitted THz power scales as the square of the radiated field, this amounts to a relative power enhancement of 20 ± 4.

THz emission from semiconductor surfaces has contributions from several mechanisms, including photocarrier effects[13–17] and nonlinear optical processes.[4,10,11] For InP, in particular, at low-excitation fluence it was shown that photocarrier acceleration in the surface depletion field dominates (at room temperature),[14] whereas bulk OR and photocarrier diffusion dominate at higher fluences, with the crossover in mechanisms occurring at fluences between $0.1-10$ μJ/cm^2.[4]

To address the question of which process is being enhanced in the present paper, the *s*-polarized THz emission from the porous sample was examined as a function of the azimuthal angle. For emission from bulk samples resulting from photocarrier effects, the generated transient current is oriented perpendicular to the surface, which cannot radiate an *s*-polarized wave,[18] and will therefore not contribute to the THz radiation for a *p-s* geometry. In the porous sample, where there is the possibility of lateral photocurrents due to the more complex surface geometry, *s*-polarized THz radiation may be generated. However, the emission would be expected to be angularly independent. The result for the porous sample is plotted, along with the data for the *p*-polarized THz emission from Fig. 2, in Fig. 3. Clearly, the *s*-polarized THz field is nonzero, and has the expected twofold rotational symmetry associated with a second-order nonlinear response from (100)-oriented InP. Moreover, the angularly independent contribution to the *s*-polarized THz field is less than 10%, indicating the *s*-polarized THz emission is primarily due to optical rectification.
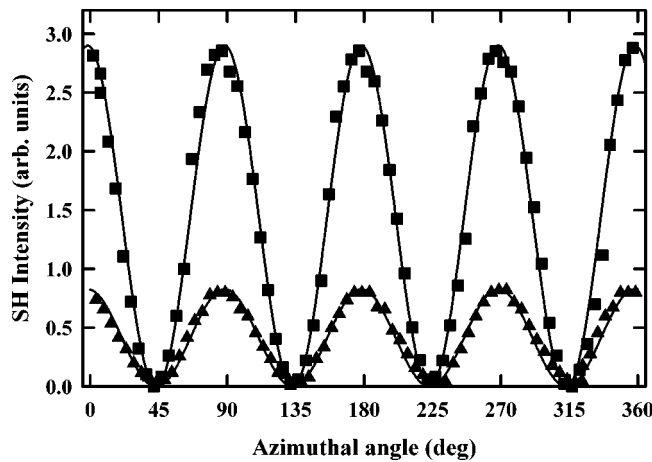
FIG. 4. Azimuthal dependence of the *p*-polarized second-harmonic intensity measured in reflection from bulk (squares) and porous (triangles) InP(100) under *p*-polarized excitation. Solid lines are qualitative fits to the data reflecting azimuthal dependence.

Measurements of the *s*-polarized emission from the bulk InP(100) show a peak detected field of approximately 0.6 ± 0.25 V/cm (maximum of the signal as a function of angle), however, the signals were close to the noise floor of our detection system. Taking the ratio of the square of the peak-detected *s*-polarized THz signals from porous relative to bulk InP gives a power ratio of 100 ± 40. The power enhancement factor is therefore attributed to the portion of the THz wave radiated by the process of optical rectification.

Optical second-harmonic generation (SHG) from bulk and porous InP(100) was also investigated. The same optical pump source was used. The Ti:Sapphire pump laser beam was passed through a polarizer to select *p*-polarized pump and incident at $45°$ on the InP samples. The pump fluence was adjusted to approximately 1 mJ/cm^2 incident on the sample surfaces. A low-pass filter was used to block the second harmonic leakage from the laser cavity prior to striking the sample surfaces. The reflected SH radiation at a 400-nm wavelength was collected using a 7.5-cm focal length lens and passed through a short-pass filter to block the fundamental beam. A UV polarizer was used to pass only the *p*-polarized second harmonic to a Hamamatsu R7518 photomultiplier tube, which was, in turn, blocked by a 400-nm interference filter to remove any further leakage of the 800-nm fundamental beam. The InP samples were rotated about their surface normal. The measured azimuthal dependence of the SH intensity is shown in Fig. 4. The solid curve is a fit to the function: $I_{SH} = a \cos^2(2\phi)$, which is expected for (100)-oriented InP. It is seen from Fig. 4 that the SH intensity measured from porous sample is 0.8 ± 0.2, or approximately three times smaller than measured from the bulk InP sample. Given the fact that the skeleton feature size in the porous network is comparable with the generated SH wavelength, significant scattering of the SH radiation in the porous network is expected. It is therefore expected that only a fraction of the total SH radiation generated in reflection, in the specular direction from the porous sample, is detected by the photomultiplier tube.

To test this assertion, in a separate experiment using 400-nm radiation, the reflection from the porous membrane was compared to that from the bulk using a variable aperture technique, where it was determined that only 10% of the reflected radiation was specularly reflected within a cone angle of 5.9×10^{-3} sr, whereas 90% of the reflected radiation was diffusely reflected. We assume that the porous InP surface is a Lambertian surface and that generated SH radiation will be completely scattered into 2π sr in the reflection (backward) direction. In our case, the effective solid angle for collecting diffusely reflected SH radiation is 0.038 sr due to the limiting aperture of the UV polarizer in the beam path. Taking this into account, it was estimated that approximately 0.86% of the total reflected SH radiation has been collected and detected in the present experiment. Correcting the measurement for scattering fraction gives a measured power ratio of SH radiation from the porous membrane relative to the bulk sample of 33 ± 7. In addition, measurements on the *s*-polarized SHG were made, where it was observed that the ratio of power in the SH beam from porous, relative to bulk was 0.48 ± 0.08. Again, correcting for the scattering losses, an estimated enhancement factor for the *p-s* geometry of 56 ± 9 was observed. This qualitatively agrees with the observation that a higher conversion efficiency results from the porous network in the *p-s* as compared to the *p-p* geometry for THz emission.

This enhancement is believed to be a result of local field enhancement within the porous network. It is well known that fields near sharp edges can be very large. The power in the SH or THz radiation scales as the input pump intensity squared, such that the output scales as the input electric field strength to the fourth power. Therefore a volumetric averaged field strength in the porous network would only have to be approximately $30^{1/4} = 2.3$ times larger than in the bulk in order to explain the results presented here. Local field enhancement is conceptually similar to focusing a pump beam to achieve higher conversion efficiencies.

At this point it is worth noting that an increased effective interaction length of the fundamental and SH or THz radiation may exist due to scattering, which would also lead to an enhancement.[2,3] We expect this effect to be minor in comparison to local field enhancement for the following reasons. First, the absorption in InP of the second harmonic beam is strong enough that the escape depth of the SH radiation limits the probed volume to a small depth. This implies that even if there were substantial scattering of the pump beam, the effective interaction length with the SH radiation is limited by the escape depth of the 400-nm light, which is much less than the optical absorption depth of the fundamental beam. For the case of THz emission, there is virtually no scattering of the THz radiation as the wavelength in this case is much larger than the characteristic sizes of the porous membrane entities. Given that the enhancement factors are qualitatively similar for THz and SHG, it seems likely that the same process governs both emissions. More work is required to demonstrate the exact contributions from scattering and local field enhancement.

In conclusion, it was found that a porous InP(100) membrane radiates approximately 20 times more power to the far infrared by optical rectification of a femtosecond Ti:Sapphire laser in comparison to bulk InP(100), at an excitation fluence of 1 mJ/cm^2. Measurements made in a *p-s* geometry indi-

cate that the primary enhancement comes from the optical rectification component to the radiated THz field. Measurements of the related process of second-harmonic generation were made on the same samples and at the same excitation fluence. As a result, approximately 30 times more power was radiated in the second-harmonic beam from the porous samples. The enhancement factor is attributed to enhancements of the local field within the porous network.

*Electronic address: rfed@ece.ualberta.ca

[1] I. M. Tiginyanu, I. V. Kravetsky, S. Langa, G. Marowsky, J. Monecke, and H. Föll, Phys. Status Solidi A **197**, 549 (2003).

[2] V. A. Mel'nikov, L. A. Golovan, S. O. Konorov, D. A. Muzychenko, A. B. Fedotov, A. M. Zheltikov, V. Y. Timoshenko, and P. K. Kashkarov, Appl. Phys. B: Lasers Opt. **79**, 225 (2004).

[3] L. A. Golovan, V. A. Mel'nikov, S. O. Konorov, A. B. Fedotov, S. A. Gavrilov, A. M. Zheltikov, P. K. Kashkarov, V. Y. Timoshenko, G. I. Petrov, L. Li *et al.*, JETP Lett. **78**, 193 (2003).

[4] M. Nakajima, Y. Oda, and T. Suemoto, Appl. Phys. Lett. **85**, 2694 (2004).

[5] D. M. Mittleman, M. Gupta, R. Neelamani, R. G. Baraniuk, J. V. Rudd, and M. Koch, Appl. Phys. B: Lasers Opt. **68**, 1085 (1999).

[6] X. C. Zhang, Phys. Med. Biol. **47**, 3667 (2002).

[7] S. Langa, J. Carstensen, M. Christophersen, H. Föll, and I. Tiginyanu, Appl. Phys. Lett. **78**, 1074 (2001).

[8] M. Reid and R. Fedosejevs, Appl. Opt. **44**, 149 (2005).

[9] P. C. M. Planken, H. K. Nienhuys, H. J. Bakker, and T. Wenckebach, J. Opt. Soc. Am. B **18**, 313 (2001).

[10] S. L. Chuang, S. Schmitt-Rink, B. I. Greene, P. N. Saeta, and A. F. J. Levi, Phys. Rev. Lett. **68**, 102 (1992).

[11] D. You, R. R. Jones, P. H. Bucksbaum, and D. R. Dykaar, J. Opt. Soc. Am. B **11**, 486 (1994).

[12] T. A. Germer, K. W. Kolasinski, J. C. Stephenson, and L. J. Richter, Phys. Rev. B **55**, 10 694 (1997).

[13] X. C. Zhang and D. H. Auston, J. Appl. Phys. **71**, 326 (1992).

[14] M. Nakajima, M. Hangyo, M. Ohta, and H. Miyazaki, Phys. Rev. B **67**, 195308 (2003).

[15] M. B. Johnston, D. M. Whittaker, A. Corchia, A. G. Davies, and E. H. Linfield, Phys. Rev. B **65**, 165301 (2002).

[16] T. Dekorsy, H. Auer, H. J. Bakker, H. G. Roskos, and H. Kurz, Phys. Rev. B **53**, 4005 (1996).

[17] J. N. Heyman, P. Neocleous, D. Hebert, P. A. Crowell, T. Mueller, and K. Unterrainer, Phys. Rev. B **64**, 085202 (2001).

[18] W. Lukosz, J. Opt. Soc. Am. **69**, 1495 (1979).